Deformation of Nanocrystalline Metals under Nanoscale Contact

F. Sansoz and V. Dupont

School of Engineering, The University of Vermont,
Burlington, VT 05405, USA, frederic.sansoz@uvm.edu

ABSTRACT

Quasicontinuum simulations have been performed to study the nanoindentation of a columnar grain boundary (GB) network in nanocrystalline Al at zero temperature. The objective was to investigate the relationship between structural evolution at GBs and incipient plasticity when the average grain size becomes smaller than the nanoindenter tip radius. A GB network made of low-angle and high-angle <110> tilt GBs was simulated by generating randomly-oriented 5-nm grains at the surface of a 200 nm-thick film. The major conclusions of this investigation are that (1) nanocrystalline GB networks cause significant softening effects at the contact interface; (2) GB movement and deformation twins are found to be the predominant deformation modes in columnar nanocrystalline Al; and (3) the cooperative grain deformation behavior is driven by the redistribution of atomic shear stress gradients between grains.

Keywords: atomistic simulation, nanoindentation, nanocrystalline aluminum, grain boundary movement

1 INTRODUCTION

The structure of a grain boundary (GB) network has a pronounced influence on the deformation of nanocrystalline metals. This observation is supported by atomistic results showing that intergranular slip and GB behavior such as GB sliding and GB migration, can vary in nanocrystalline metals based on the type of structural units and point defects present in the GBs [1]. In addition, grain growth via GB movement mechanisms has been observed in nanocrystalline Al at room temperature under in-situ TEM nanoindentation [2]. Similarly, recent evidence of rapid-grain growth at room and cryogenic temperatures has been found in nanocrystalline Cu under micro-indentation [3]. This abnormal GB behavior is not fully understood in nanocrystalline metals. Furthermore, the effect of nanoindentation on grain size evolution in nanomaterials needs to be fundamentally addressed.

In the present paper, we report on the nanoindentation of a columnar GB network in nanocrystalline Al simulated by hybrid continuum/atomistic modeling. This investigation aims at understanding the relationship between structure evolution at GBs and incipient plasticity for indenter tips significantly larger than the average grain size. The nanoindentation simulations were performed by quasicontinuum method at zero temperature. A GB network made of vicinal and high-angle <110> tilt GBs was studied by generating randomly-oriented nanosized grains at the surface of a 200 nm-thick film. This study shows for the first time the simulation of growth, coalescence and disappearance of nanosized grains by nanoindentation in the athermal limit.

Section 2 provides the details of the computational set up. In Section 3, we present and discuss the nanoindentation response and underlying deformation mechanisms of both single crystal and nanocrystalline Al films.

2 COMPUTATIONAL PROCEDURE

Both film and indenter geometries were simulated using the quasicontinuum method [8]. This technique provides the solution of equilibrium atomic configurations by energy minimization, given externally imposed forces or displacements; and does not explicitly represent every atom in the simulation cell. In fact, the regions of small deformation gradients are treated as continuum zones by finite element method. In the present model, only the region at the interface between indenter tip and substrate was modeled by full atomistic. The indenter was represented by an Al single crystal cylinder with a radius of 15 nm. The indenter axis was oriented along the $[1\bar{1}0]$ direction with a <100> direction of indentation. The film dimensions were 400nm × 200nm × 0.286nm. The size of the full atomistic zone was 50nm × 25nm. A periodic boundary condition was imposed in the out-of-plane direction. Two structures were studied for the film. The first structure consisted in a single crystal with a (111) surface and a $[1\bar{1}0]$ out-of-plane direction. The second structure investigated was a polycrystal constructed as follows. Reference atoms were placed randomly in the sample at an average distance equal to the desired grain size and GBs were formed by a Voronoi construction which was based on a constrained-Delaunay connectivity scheme. For this study, the average grain size was 5 nm.

Each grain was assigned a common tilt axis along $[1\bar{1}0]$ and random in-plane orientation. Starting from the reference atom, the other atoms of the grains were added according to the Bravais lattice cell [9]. We fixed the surface orientation of the first grain of the film in contact with the indenter to match that of the single crystal model i.e., [111]. Furthermore, in order to avoid the discontinuities in the energy state at the continuum/atomistic frontier, the latter was modelled using a single crystal with the orientation of the single crystal model described above. A total number of 50 grains were fully represented in the atomistic zone under the indenter. We used an embedded-atom-method (EAM) potential for Al by Voter and Chen [10]. The energy minimization was performed at zero temperature by conjugate gradient method. The sample was first relaxed under zero force lattice static condition in order to obtain the lowest state of energy. The indenter was kept completely rigid and we fixed the bottom of the film. After this step, the atoms of the indenter were displaced by increment of 0.75Å until the depth of penetration reached 7.5 nm. Energy minimization was performed between each loading steps. The total force on the nanoindenter was calculated by adding the out-of-balance forces acting in the contact area and projected along the direction of indentation.

In order to detect the presence of planar defects and GB structure evolution with respect to the elastically deformed crystal domain, the centrosymmetry parameter proposed by Kelchner et al. [11] was used. Our coloring scheme for this parameter is as follows. Atoms in perfect fcc sequence are colored in blue, those with a hcp structure or representing a stacking fault are colored in green, and all other, non-coordinated atoms are colored in red. The local stress tensor of the i^{th} atom $\tilde{\sigma}_i$ was calculated in the full atomistic region using the formula provided by Lilleodden et al. [6], which can be simplified as follows:

$$\sigma_i^{\alpha\beta} = \frac{1}{\omega_i^0 \, Det[F_i^{\alpha\beta}]} \left\{ \frac{1}{2} \sum_j \left(-\frac{1}{r} \frac{\partial \varphi}{\partial r} \right) r^\alpha r^\beta \Big|_{r=r_{ij}} \right\} \qquad (1)$$

where α and β are the Cartesian coordinates, ω_i^0 is the undeformed atomic volume of the i^{th} atom, $Det[F_i^{\alpha\beta}]$ is the determinant of the deformation gradient, φ is the interatomic potential, and r_{ij} is the distance between i^{th} and j^{th} atoms. Note that the kinetics terms have been eliminated in equation (1) as compared to ref. [6]. In this equation, the use of the determinant of the deformation gradient has been shown to provide improved accuracy for the calculation of deformed atomic volumes. Furthermore, the principal shear stress was calculated for each atom using the components of the atomic-level stress tensor $\tilde{\sigma}_i$ described above, using the formula provided in ref. [12].

3 RESULTS AND DISCUSSION

3.1 Nanoindentation Response

The response of both single crystal and nanocrystalline thin films during simulated nanoindentation are represented in Fig. 1. This figure clearly shows that the polycrystal model is significantly softer than the single crystal case. As shown below, this behavior can be interpreted in terms of the GB sliding process occurring at an early indentation stage. However, the analysis of deformation mechanisms will also demonstrate that more complex mechanisms such as grain growth and shear banding, take place at larger imposed deformation.

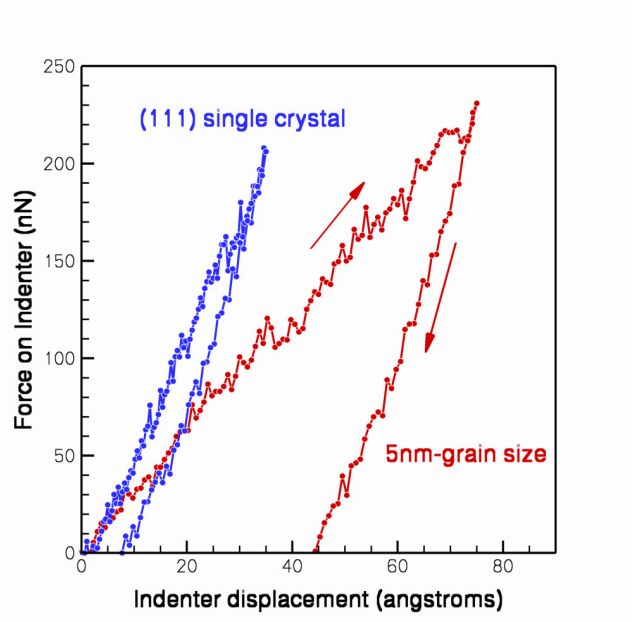

Figure 1: Nanoindentation response of single crystal and 5nm-grain size Al thin films simulated with a 15 nm-radius indenter. Significant softening effects can be seen in the response of the nanocrystalline thin film.

3.2 Atomic-Level Stress Evolution in Relation to the Deformation Mechanisms

Our simulation of indentation of the single crystal film was found to be in good agreement with the results of the literature. It was observed for example that the onset of plasticity in the film occurs by nucleation of <112> dislocations emanating from the contact interface. Our model also accurately predicted the effects of adhesion and interfacial friction at the early stage of indentation. These effects were found to displace the maximum value of principal shear stress closer to the contact interface, in accordance with the elastic theory [12].

The deformation mechanisms of nanoindentation strongly vary in the presence of GB networks as shown in Fig. 2. A large number of <112> partial dislocations and deformation twins, which were often nucleated in grains that are not directly in contact with the indenter, can be observed in this figure. Consistent to the existing literature, the GB structure dominates the dislocation nucleation process and also serves as dislocation sink. Additionally, we found that the partial dislocations nucleated preferentially from triple-junctions in order to accommodate GB sliding. GB sliding occurs at early stage due to GB atom shuffling. This mechanism is well-known and has been detailed elsewhere [1,4]. Our simulation also shows that GB sliding is associated with significant grain rotation and results in the formation of thin shear bands. Figure 3a shows the formation of the first shear band. It is important to note in this figure that the extension of the shear band into grain 2 is achieved by intragranular slip in the prolongation of the interface between grains 3 and 4. Furthermore, a deformation twin was grown in grain 2 from adjacent partial dislocations emitted by the same interface. For larger depths of indentation, significant GB movement was observed and, to some extent, linked to the twin growth process. GB movement in association with grain rotation caused cooperative grain behaviors as shown in Fig. 3a. In this example, it is possible to observe simultaneous events of grain coalescence (grains 2 and 3), disappearance (grain 1) and growth (grains 4 and 5).

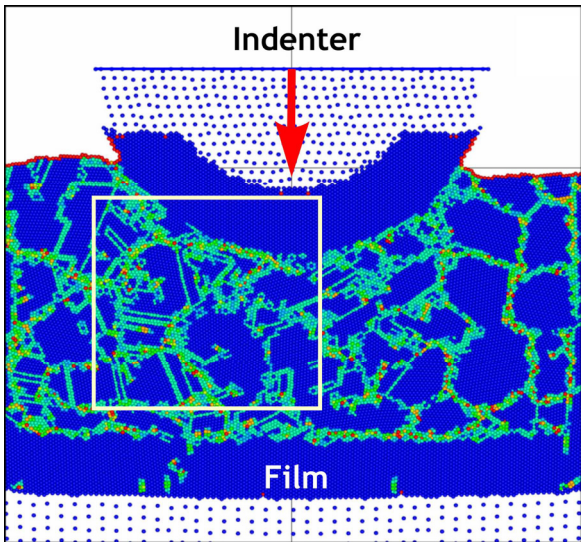

Figure 2: Quasicontinuum simulation of a grain boundary network after nanoindentation. The average grain size before indentation was 5 nm. Atoms are colored with respect to their crystal symmetry. See text for details.

In order to gain additional insights into the role played by the stress on the deformation mechanisms, we have examined the evolution of principal shear stress obtained at atomic-level for different steps of indentation. Figure 3b shows the evolution of the atomic-level shear stresses during indentation. Note that each stress map corresponds to the microstructure shown in Fig. 3a. We can clearly see in this figure that the principal shear stresses are higher in the GB area as compared to the grain interior before indentation. This observation seems to explain why dislocations were found to nucleate preferentially on GB sites. More importantly, our simulation also reveals that, after indentation, grain rotation causes significant decrease of the gradient of principal shear stress across the interfaces. At the maximum indentation depth corresponding to the maximum applied load, it is even difficult to relate the stress pattern to the grain structure because of the significant redistribution of principal shear stresses.

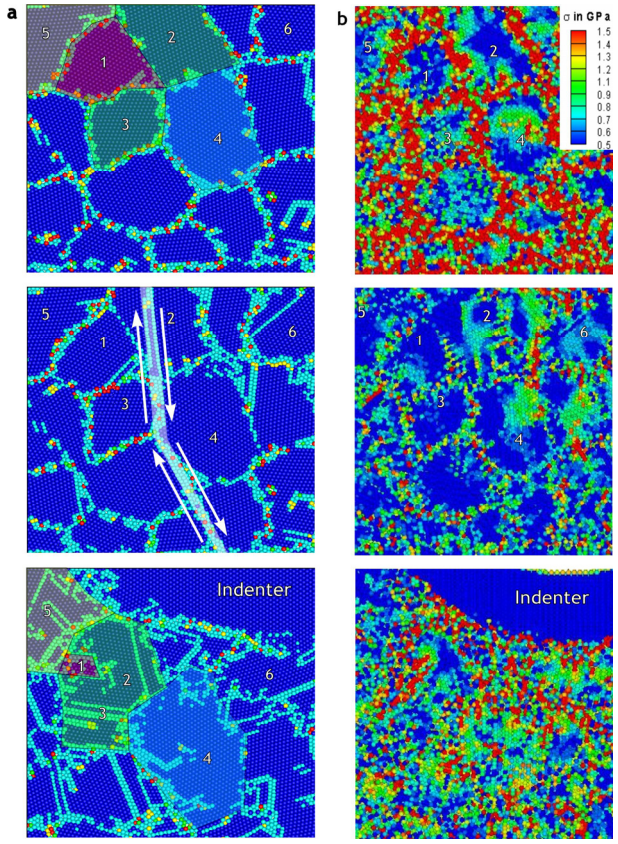

Figure 3: Magnified view of the area framed in Fig. 2 shown at different applied loads. (a) Shear banding and cooperative grain boundary processes occurring below the indenter. (b) Distribution of the principal shear stress calculated at atomic level.

4 CONCLUSIONS

The nanoindentation of a columnar GB network in 5nm grain-sized Al has been examined by hybrid continuum/atomistic simulations. This study shows for the first time the atomistic simulation of growth, coalescence and disappearance of nanosized grains by nanoindentation in the athermal limit. In addition, the major findings of this investigation can be summarized as follows: (1) nanocrystalline GB networks profoundly impact on the nanoindentation response and cause significant softening effects at the contact interface; (2) GB movement and deformation twins are found to be the predominant deformation modes in columnar nanocrystalline Al; here we found that shear bands form by GB sliding and intragranular slip, and crystal growth by grain rotation and coalescence; and (3) the cooperative GB deformation is found driven by the redistribution of atomic-level shear stress gradients between grains.

ACKNOWLEDGEMENTS

This study was performed under the auspices of the Vermont Experimental Program to Stimulate Competitive Research (VT EPSCoR) under grant number NSF EPS 0236976.

REFERENCES

[1] F. Sansoz and J. F. Molinari, *Acta Mater* **53**, 1931 (2005).
[2] M. Jin, A. M. Minor, E. A. Stach and J. W. Morris Jr., *Acta Mater* **52**, 5381 (2004).
[3] K. Zhang, J. R. Weertman and J. A. Eastman, *Appl. Phys Lett.* **87**, 061921 (2005).
[4] D. Feichtinger, P. M. Derlet and H. Van Swygenhoven, *Phys Rev B* **67**, 024113 (2003).
[5] X. L. Ma and W. Yang, *Nanotechnology* **14**, 1208 (2003).
[6] E. T. Lilleodden, J. Zimmerman, S. M. Foiles and W. D. Nix*, J. Mech. Phys. Solids* **51**, 901 (2003).
[7] J. Chen, W. Wang, L. H. Qian and K. Lu, *Scripta Mater* **49**, 645 (2003).
[8] R. Miller, E. B. Tadmor*, J. Comput. Aided Mater. Des*. **9**, 203 (2002).
[9] A. Brokman and R. W. Balluffi*,* Acta Metall. **29**, 1703 (1981).
[10] A. F. Voter and S. P. Chen*,* Mat. Res. Soc. Symp. Proc. **82**, 175 (1987).
[11] C. L. Kelchner, S. J. Plimpton and J. C. Hamilton*, Phys Rev B* **58**, 11085 (1998).
[12] K. L. Johnson, K. Kendall and A. D. Roberts, *Proc R Soc London A* **324**, 301 (1971).
[13] A. Hasnaoui, H. Van Swygenhoven and P. M. Derlet, *Phys. Rev. B* **66**, 184112 (2002).
[14] L. M. Dougherty, I. M. Roberston, J. S. Vetrano, *Acta Mater* **51**, 4367 (2003).